The Edge Focusing Effect of Injection and Extraction Orbit Bumps in the Fermilab Booster *

C. Ankenbrandt, W. Chou, A. Drozhdin, J. Lackey, P. Lucas, F. Ostigay, M. Popovic, ...

Fermi National Accelerator Laboratory

P.O. Box 500, Batavia, Illinois 60510

June 9, 2003

Abstract

The Fermilab Booster is a bottleneck limiting the proton beam intensity in the accelerator complex. A study group has been formed in order to have a better understanding of this old machine and seek possible improvements [1, 2]. The work includes lattice modeling, numerical simulations, bench measurements and beam studies. Based on newly obtained information, it has been found that the machine acceptance is severely compromised by the horizontal injection orbit bump located at Long01 straight section (SS) of accelerator and by two vertical extraction bumps (dogleg) located at Long03 and Long13 SS. This, accompanied by emittance dilution from space charge at injection, is a major cause of the large beam loss at the early stage of the cycle. Measures to tackle this problem are being pursued.

1 Introduction

The Fermilab Booster is a 30 years old machine and the only machine at Fermilab that has never been upgraded. It is the bottleneck in the accelerator complex limiting the proton beam intensity. The linac upstream from the Booster can deliver 5 times more protons than it does now. The Main Injector downstream from the Booster can also accept 5 times more protons. However, the Booster, which sits in between, can provide no more than $6 \cdot 10^{12}$ protons per cycle. Otherwise the loss would be prohibitive. Most of the losses (about $25 - 30\%$) occur at the early stage of the cycle; in particular during the first few ms. (The cycle is 66.7 ms). In order to understand the cause of the early loss, a study group was formed about 6 months ago. It launched a systematic investigation on the Booster. A comprehensive lattice model using MAD is established. The space charge codes ESME (authored by J. MacLachlan) and ORBIT (authored by J. Holmes) are employed (the results of these calculations are not included in this paper). With the help of the Proton Source Department and other departments/divisions, a series of beam studies and magnet field measurements are also carried out.

2 Perturbation on linear optics: the Dogleg Effect

One surprise in this study is that the linear optics of the Booster is significantly perturbed by the edge focusing of the injection and extraction orbit bumps. As can be seen in Figure 1, in the horizontal

*Work supported by the Universities Research Association, Inc., under contract DE-AC02-76CH00300 with the U. S. Department of Energy.

plane, the maximum beta function is increased from 33 m to 47 m, maximum dispersion from 3 m to 6 m; in the vertical plane, the maximum beta from 20 m to 26 m.

The relationship between the coordinates at the entrance and exit faces of the sector (wedge) bending magnet are given by the transport matrix equations:

$$\begin{pmatrix} X_f \\ X'_f \\ Y_f \\ Y'_f \\ \Delta P/P \end{pmatrix} = M \times \begin{pmatrix} X_i \\ X'_i \\ Y_i \\ Y'_i \\ \Delta P/P \end{pmatrix} + \begin{pmatrix} \frac{10^3 F_p L}{2(1+\frac{\Delta P}{P})} \\ \frac{10^3 F_p}{1+\frac{\Delta P}{P}} \\ 0 \\ 0 \\ 0 \end{pmatrix}, \tag{1}$$

where

$$M = \begin{pmatrix} cos(F_p) & \frac{Lsin(F_p)}{F_p} & 0 & 0 & -\frac{10^3(1-cos(F_p))L}{F_p} \\ -\frac{F_p sin(F_p)}{L} & cos(F_p) & 0 & 0 & -10^3 sin(F_p) \\ 0 & 0 & 1 & L & 0 \\ 0 & 0 & 0 & 1 & 0 \\ 0 & 0 & 0 & 0 & 1 \end{pmatrix}, \tag{2}$$

with

$$F_p = -\frac{B(kG) \cdot L(m)}{33.356405 \cdot P(GeV/c)} = \theta. \tag{3}$$

θ is a bending angle for equilibrium particle.

As seen from equation 2 a horizontal bending sector magnet has focusing effect in the horizontal plane ($m21 \neq 0$) and it does not have focusing effect in the vertical plane (m43=0).

Rectangular bending magnet can be simulated by a sector bending magnet and two magnetic wedges from both sides of magnet (Figure 2). Focusing effect of wedges is calculated as:

$$X'_f = X'_i + \frac{B(kG) \cdot X_i \cdot \frac{F_p}{2}}{33.356405 \cdot P(GeV/c)} = X'_i + K \cdot X_i. \tag{4}$$

$$Y'_f = Y'_i - \frac{B(kG) \cdot Y_i \cdot \frac{F_p}{2}}{33.356405 \cdot P(GeV/c)} = Y'_i - K \cdot Y_i. \tag{5}$$

This eliminates focusing in the horizontal plane and causes focusing in the vertical one. The edge focusing strength of a bending magnet is:

$$K = -\frac{\theta^2}{L}. \tag{6}$$

Both sector and rectangular bending magnets produce focusing effect in only one plane, and sign of focusing does not depend on the sign of magnetic field (Figure 2). Effect is always focusing. These two circumstances do not permit to compensate focusing effect locally by a quadrupole corrector located close to the magnet or by a magnet with different sign of magnetic field.

For the Booster doglegs, L is small (0.25 m) and θ is large (60 mrad). There are two doglegs, each with 4 bending magnets (Figure 3). The focusing effects are additive, giving rise to a significant amount of extra focusing (0.115 m-1, close to one main magnet which has 1/f = 0.157 m-1) and leading to a big perturbation to the linear lattice. Both the injection orbit bump (horizontal bend) and extraction doglegs (vertical bend) are rectangular bends. Therefore, their edge focusing acts in

the non-deflecting plane. That is, vertical for the injection orbit bump and horizontal for the dogleg. The former is pulsed (pulse length about 60μs), while the latter is DC. Hence, the doglegs cause more damage to the beam.

This effect was quickly confirmed in a beam study. The measured tune shift (Figure 4) and dispersion perturbation (Figure 5) are in good agreement with the MAD prediction. When one of the doglegs was removed (Figure 6) in a machine experiment, the transfer efficiency showed a considerable improvement (Figure 7). A milestone of the MiniBooNE neutrino program ($5 \cdot 10^{16}$ protons per hour) was reached.

Several methods were suggested to mitigate the effect of extraction bump magnets: - quadrupole correction; - using different pole-face rotated magnets; - increase length of magnets and distance between them. Some of these solutions are shown below.

The first two methods: quadrupole correction, and using different pole-face rotated magnets for edge focusing effect compensation are very similar to each other, because introduction of pole-face rotation is equivalent to addition of quadrupole lens. This method can be used for the machine which is under design. But for the existing accelerator, like Fermilab Booster, it is impossible to find space for installation of correctors in optimal positions.

Using 3-magnet extraction bump (Figure 8) allows to decrease the total bending angle of the magnets and permits to decrease horizontal β by 7% and dispersion from 6 m to 5 m (Figure 9). This method may be used as a short term solution for Booster.

The most effective way to mitigate edge focusing effect is based on the increasing distance between magnets, that permits to reduce bending angle (Figure 10, 11 and 12). This allows to decrease horizontal β by 12% and dispersion by 20% in the Booster if space between magnets in both Long03 and Long13 straight sections is increased by 0.2 m, and horizontal β by 29% (Figure 13) and dispersion by 75% if space is increased by 0.56 m (Figures 14, 15, 16 and 17). If this is done in the Long03 SS only it reduces horizontal β by 15% and dispersion by 47%. Using 3-magnet extraction bump for this distance between magnets gives additional reduction of β_x by 3% and dispersion by 5%. This reconstruction will be done during the summer shutdown as a short-term solution to solve the problem.

As a long term solution the new design of injection and extraction was proposed with increased distance between magnets in the injection bump and with extraction bump used only at the accelerator top energy with extraction septum located behind the envelope of the beam at injection (Figure 18). The horizontal and vertical β functions and horizontal dispersion at injection and extraction are shown in Figure 19. The lattice function perturbations are reasonably small in this case. Unfortunately this solution requires sufficient amount of design and construction work and is pretty expensive.

Maximum value of $\beta_{x,y}$ and dispersion at injection for different solutions of injection and extraction in the Booster are presented in Table 1.

	$\Delta\beta_x$	$\Delta\beta_y$	ΔD	$\Delta\nu_x$	$\Delta\nu_y$
	%	%	%		
without injection and extraction bumps	100	100	100	0.000	0.000
with existing injection and extraction bumps	136	125	195	0.069	0.011
without extraction bump at Long13	118	124	144	0.032	0.027
distance between magnets increased by 0.56 m at Long03 and Long13	107	124	120	0.012	0.015
3-magnet extraction bumps with distance between magn. increased by 0.56 m at Long03 and Long13	104	126	114	0.006	0.032
distance between magnets increased by 0.56 m at Long03	121	124	148	0.037	0.013
3-magnet extraction bumps with distance between magnets increased by 0.56 m at Long03	118	125	143	0.034	0.019
new injection and extraction schemes	104	117	111	0.003	0.024

Table 1: Maximum of β_x, β_y, dispersion and betatron tune deviation at injection for different solutions of injection and extraction schemes in the Booster. Betatron tune without injection and extraction bumps is $\nu_x = 6.70$, $\nu_y = 6.80$.

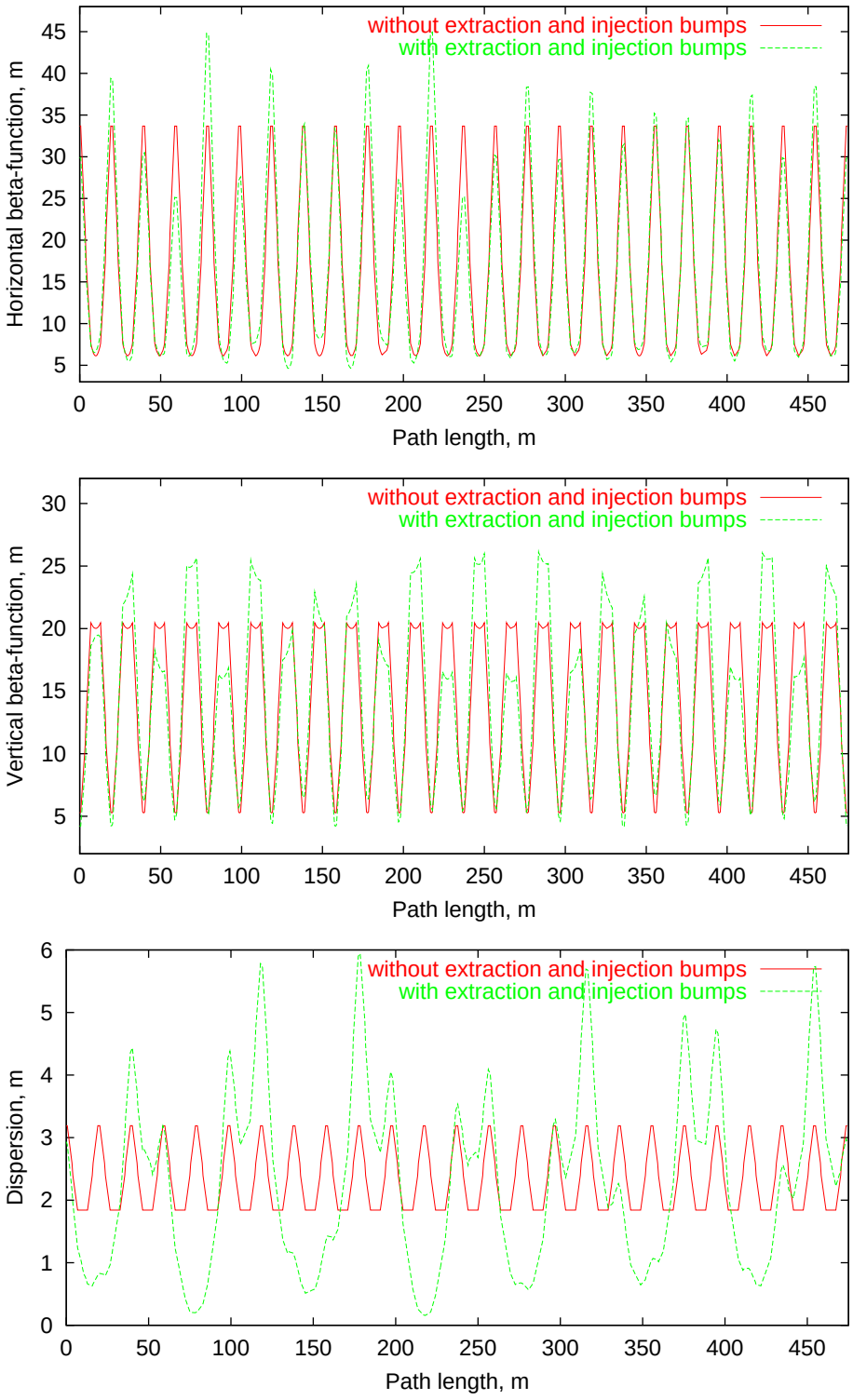

Figure 1: Fermilab Booster horizontal (top), vertical (middle) β functions and horizontal dispersion (bottom) at injection with and without injection bump at “long 01” straight section and extraction bumps at “long 03” and “long 13” straight sections.

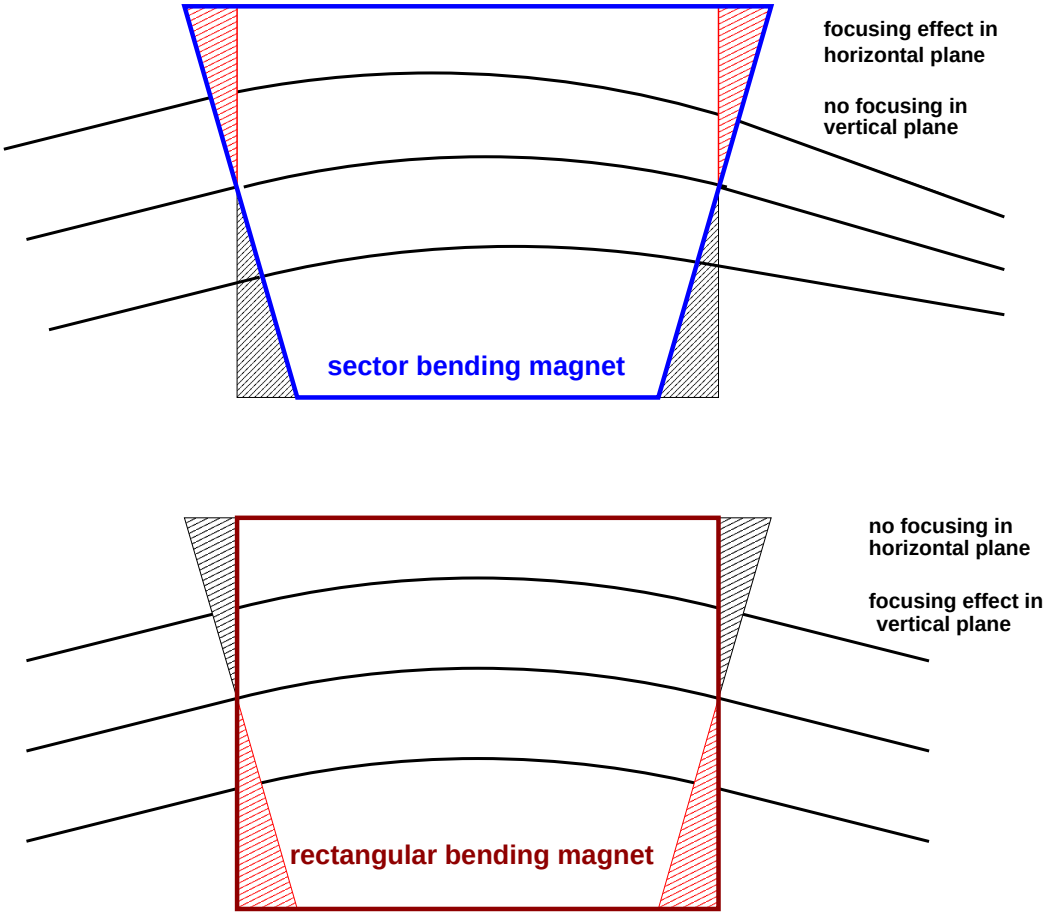

Figure 2: Focusing effect of the “sector” and “rectangular” bending magnets.

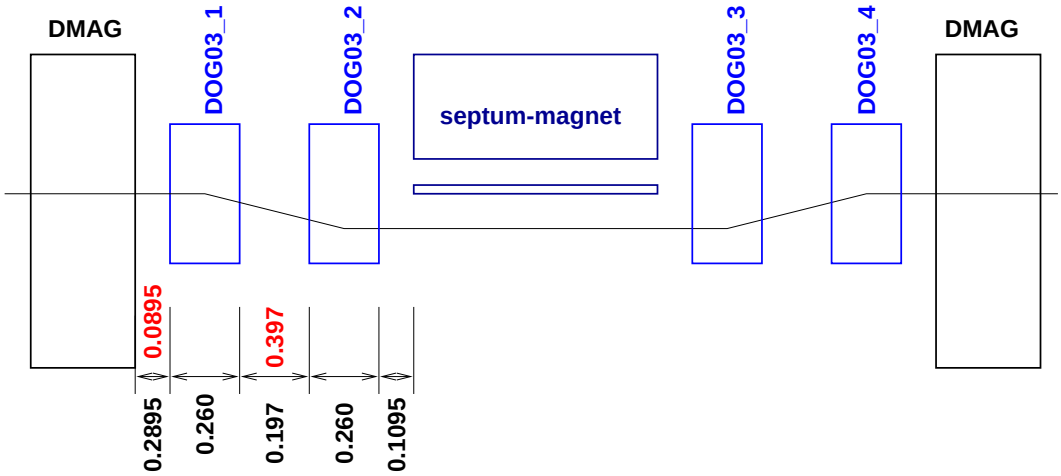

Figure 3: DogLeg bump magnets location in the Booster Long-03 straight section.

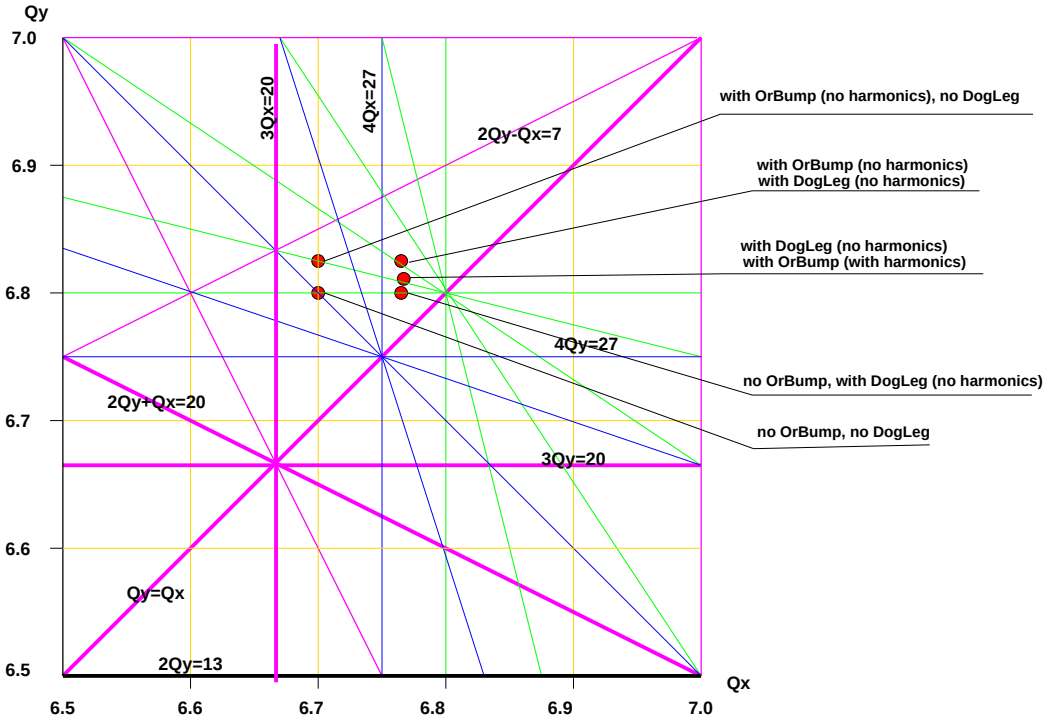

Figure 4: Fermilab Booster betatron oscillation tune at injection.

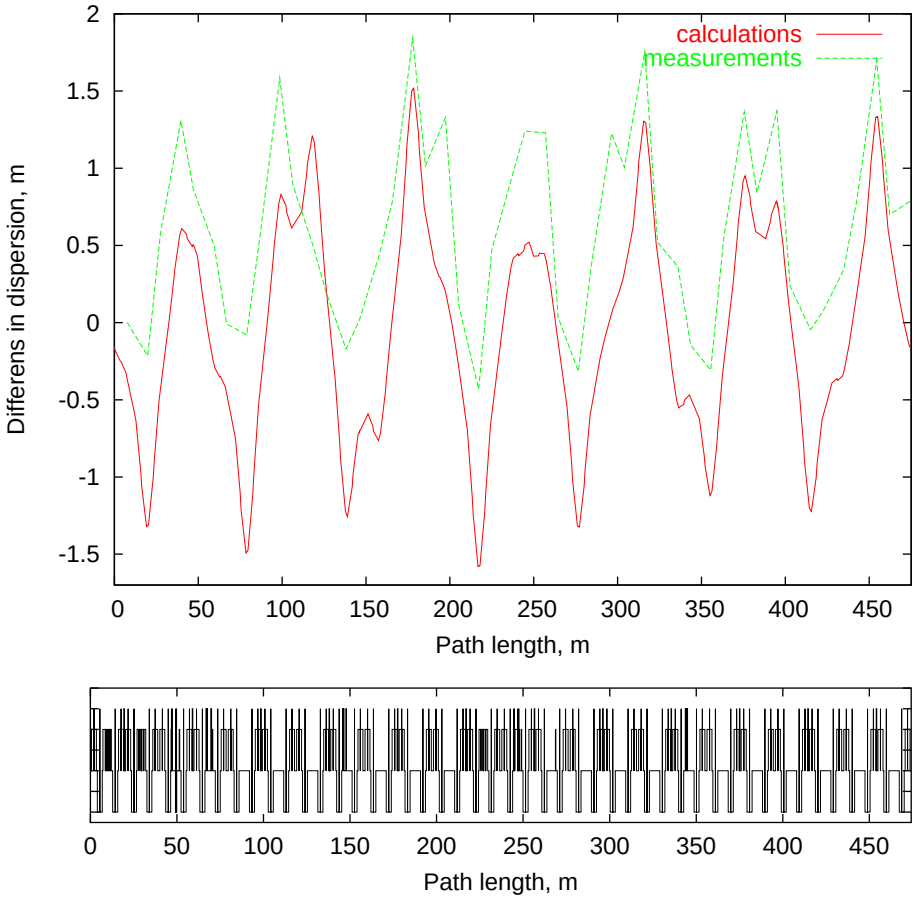

Figure 5: Measured and calculated (MAD) difference in horizontal dispersions at injection with and without extraction bump at “long 13” straight section.

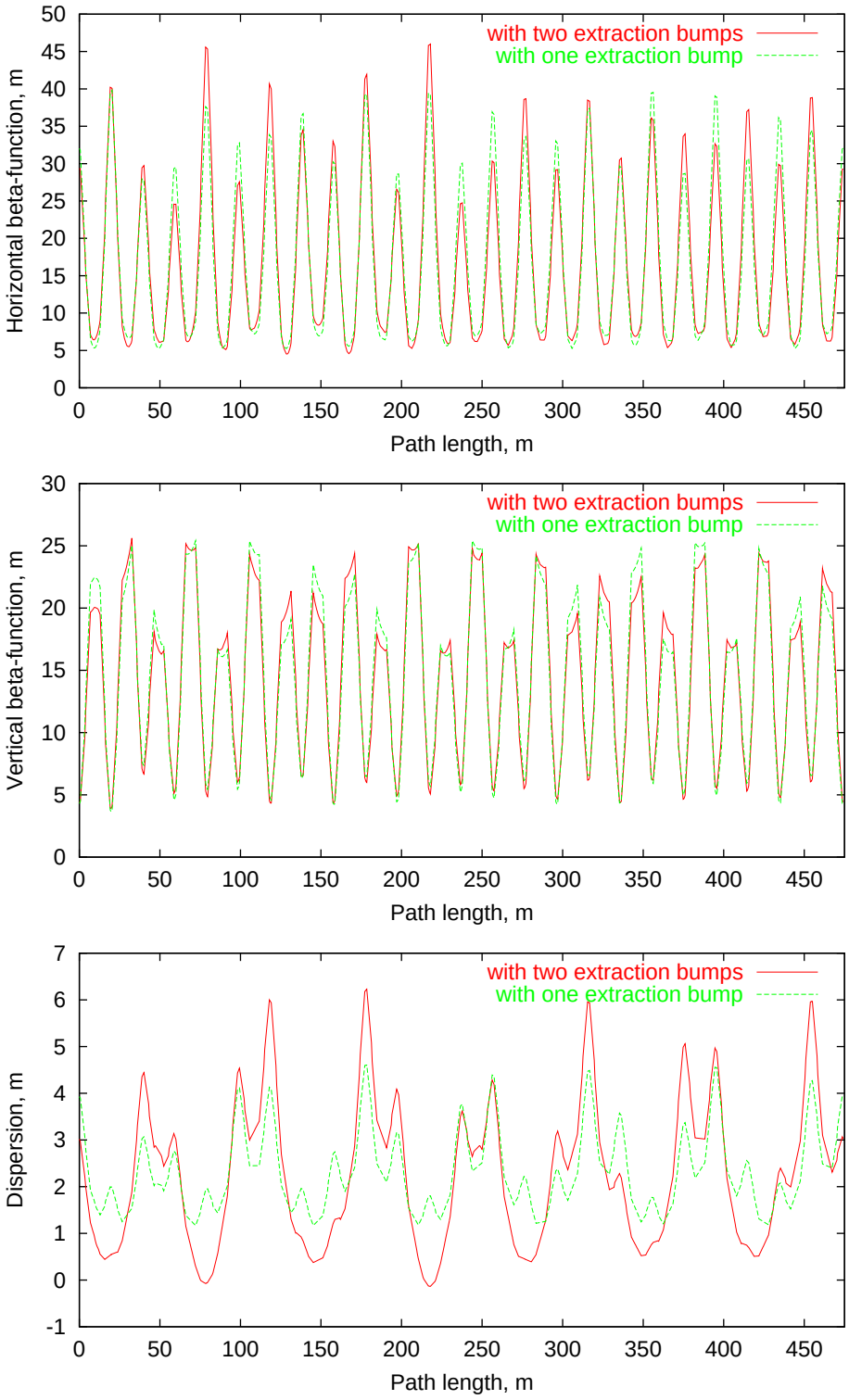

Figure 6: Fermilab Booster horizontal (top), vertical (middle) β functions and horizontal dispersion (bottom) at injection with one and two extraction bumps.

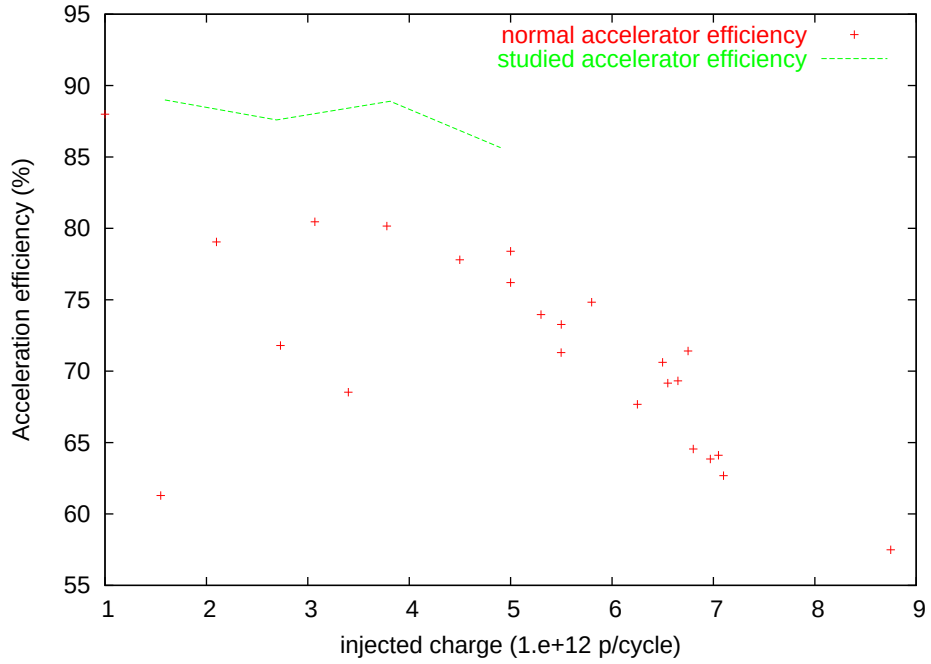

Figure 7: Transfer efficiency measured at normal Booster operation with two extraction bumps at Long03 and Long13, and in a machine experiment with only one dogleg bump at Long03 .

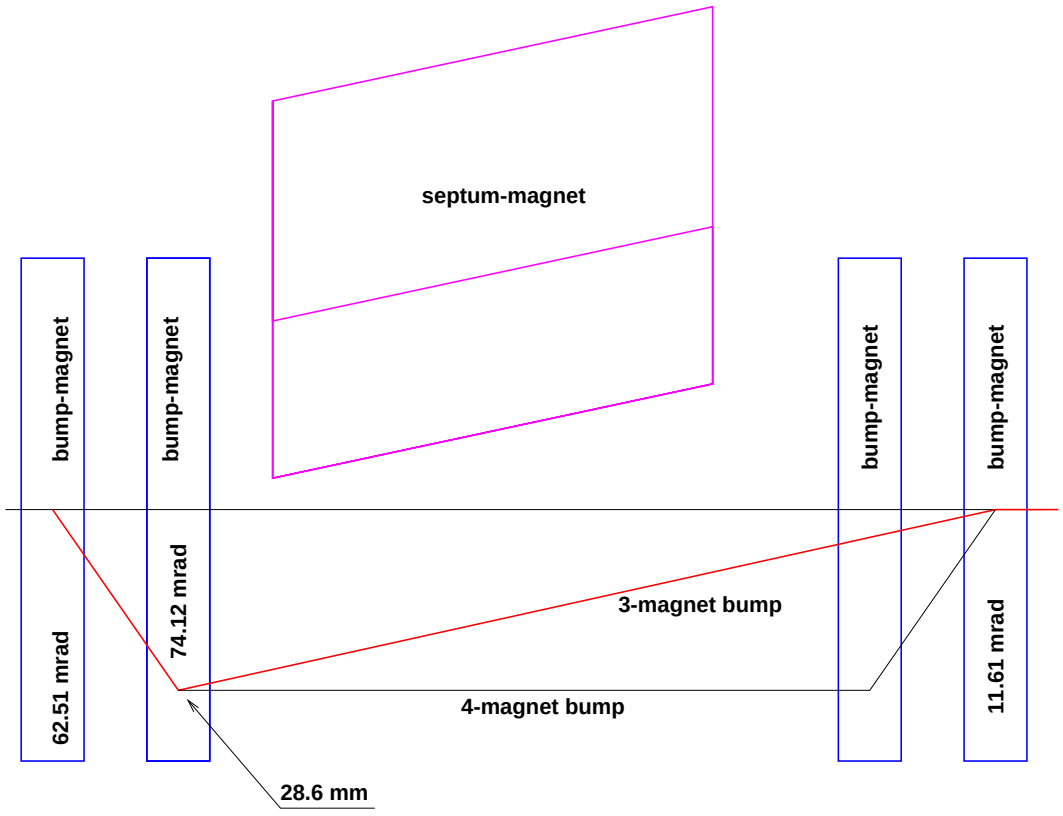

Figure 8: 3-magnet DogLeg bump.

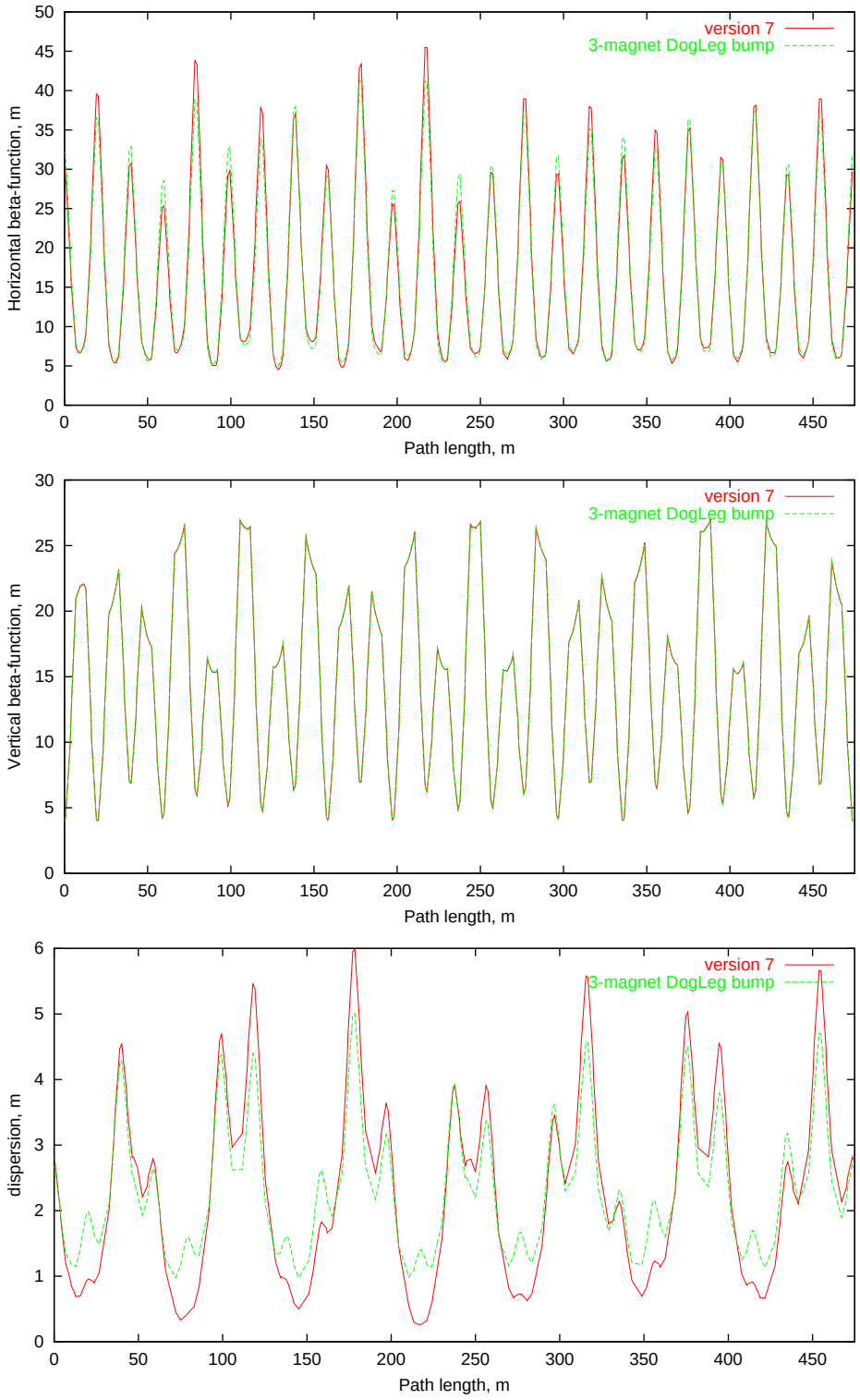

Figure 9: Fermilab Booster horizontal (top), vertical (middle) β functions and horizontal dispersion (bottom) at injection for with 4-magnet and 3-magnet DogLeg bump at Long03 and Long13.

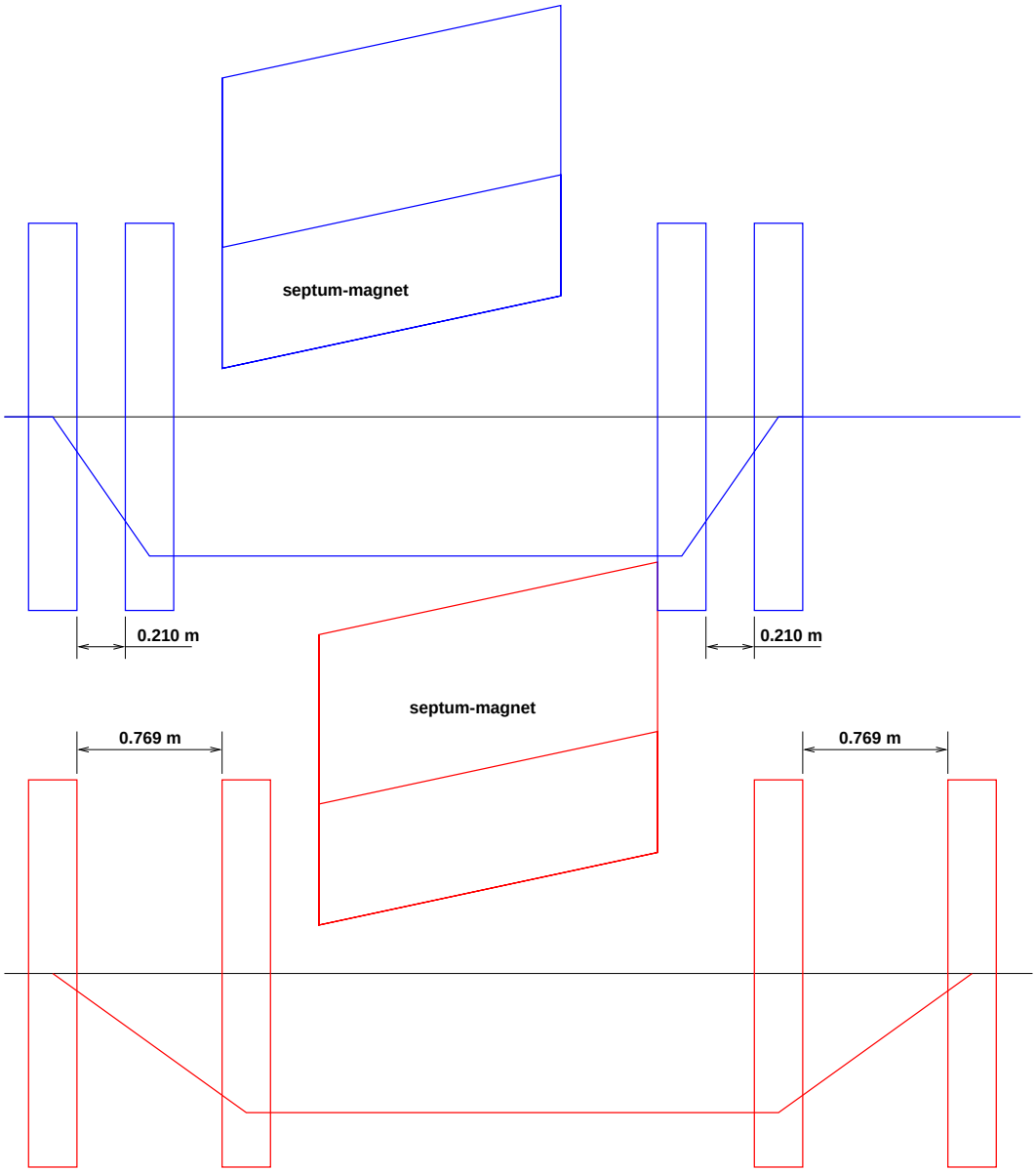

Figure 10: DogLeg bump with space between magnets increased by 0.56 m.

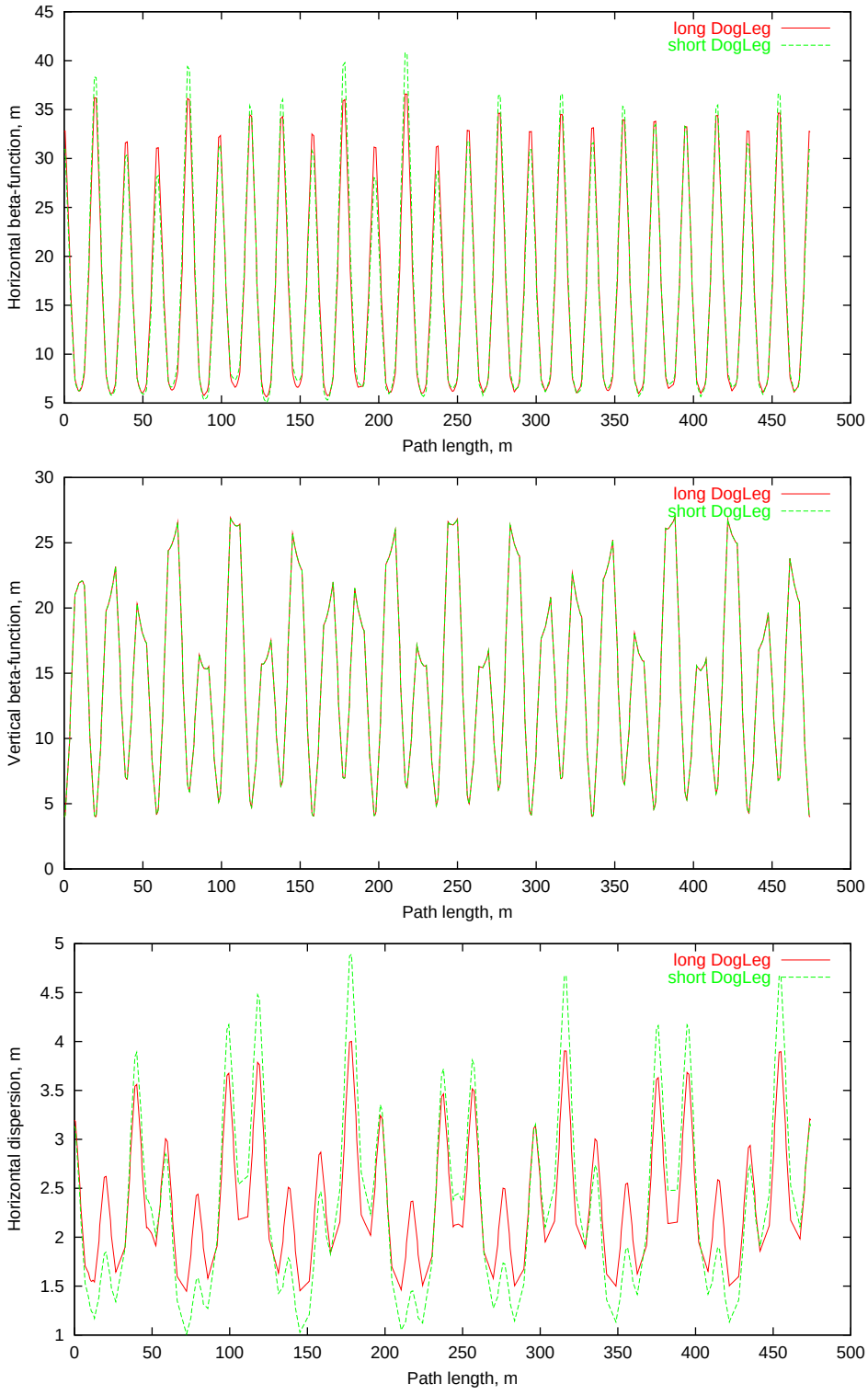

Figure 13: Fermilab Booster horizontal (top), vertical (middle) β functions and horizontal dispersion (bottom) at injection with injection bump at "long 01" straight section and with extraction bumps at "long 03" and "long 13" straight sections, with "short" distance between DogLeg magnets and with distance increased by 0.2 m.

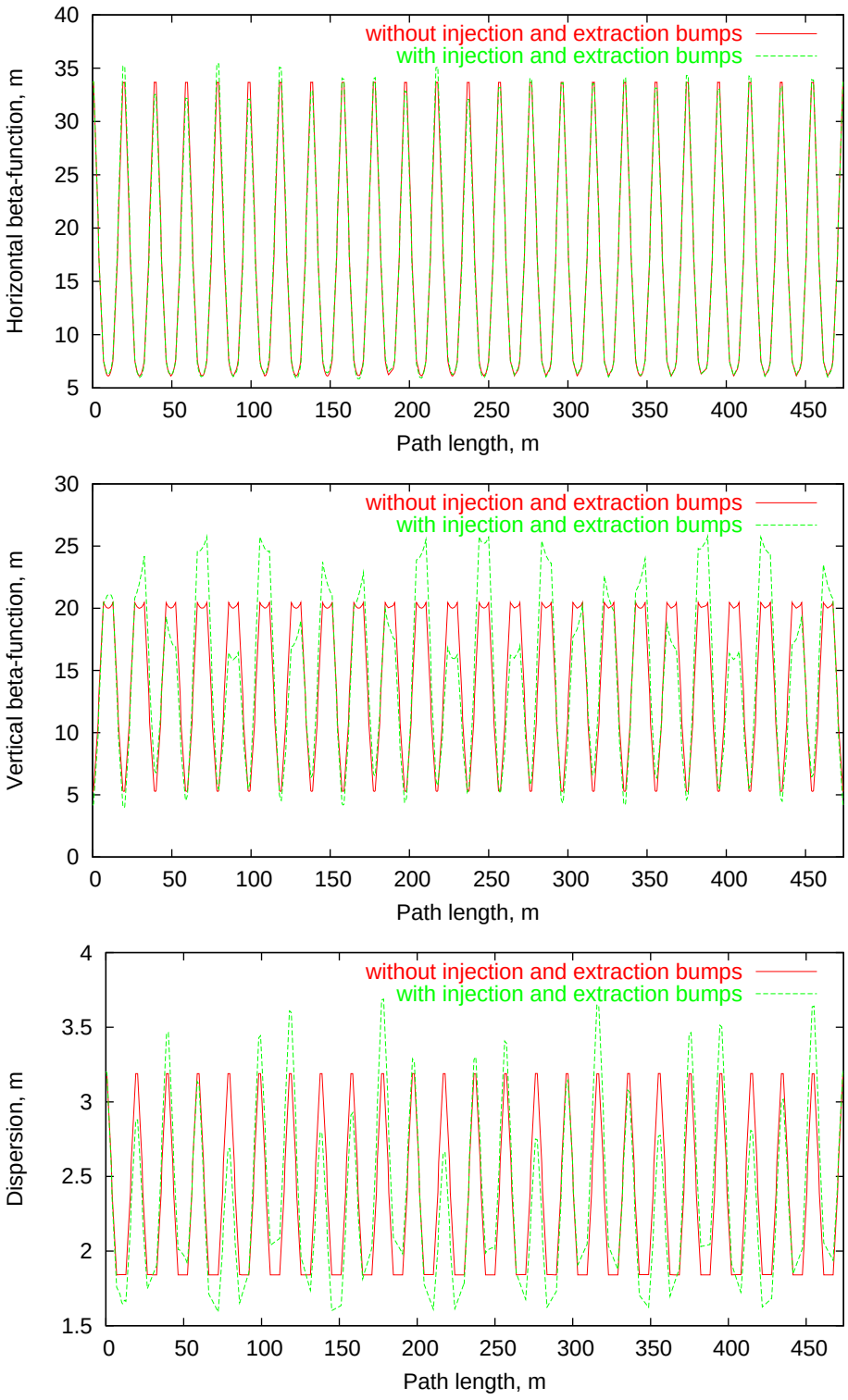

Figure 14: Fermilab Booster horizontal (top), vertical (middle) β functions and horizontal dispersion (bottom) at injection without injection and extraction bumps, and with injection bump and with DogLeg bump at Long03 and Long13 with space between magnets increased by 0.56 m.

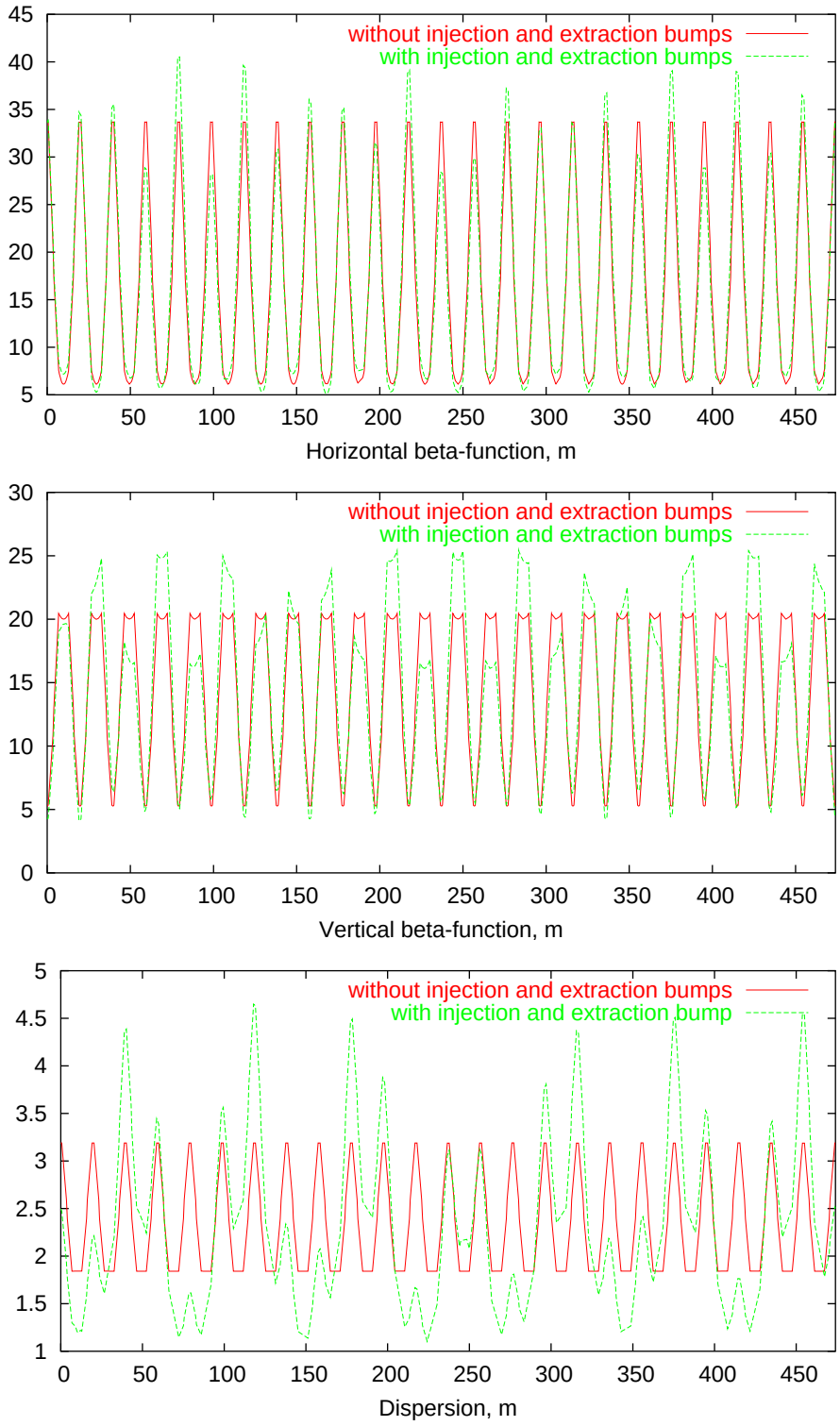

Figure 15: Fermilab Booster horizontal (top), vertical (middle) β functions and horizontal dispersion (bottom) at injection without injection and extraction bumps, and with injection bump and with DogLeg bump at Long03 with space between magnets increased by 0.56 m and old bump at Long13.

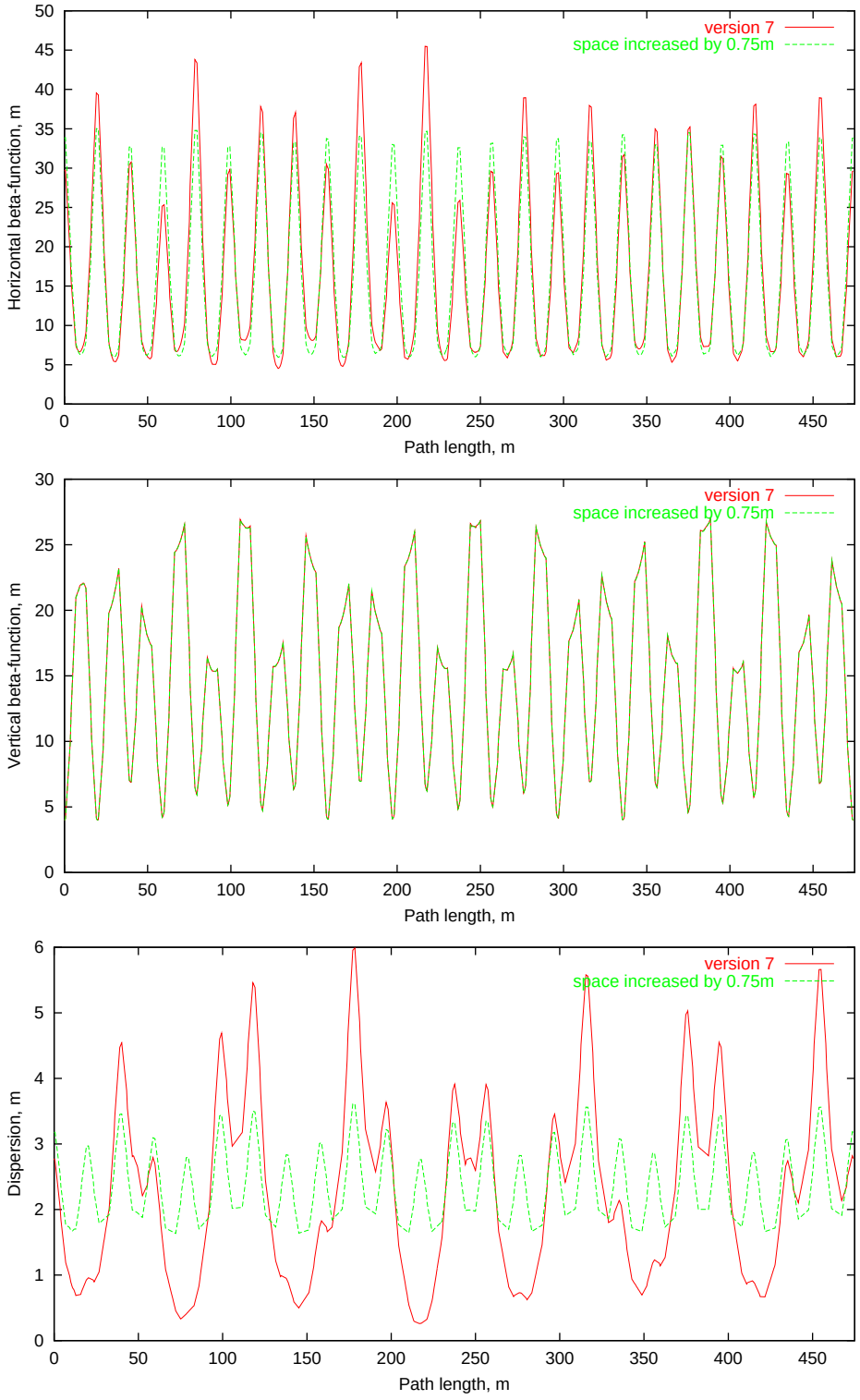

Figure 16: Fermilab Booster horizontal (top), vertical (middle) β functions and horizontal dispersion (bottom) at injection with "short" distance between DogLeg magnets and distance increased by 0.75 m.

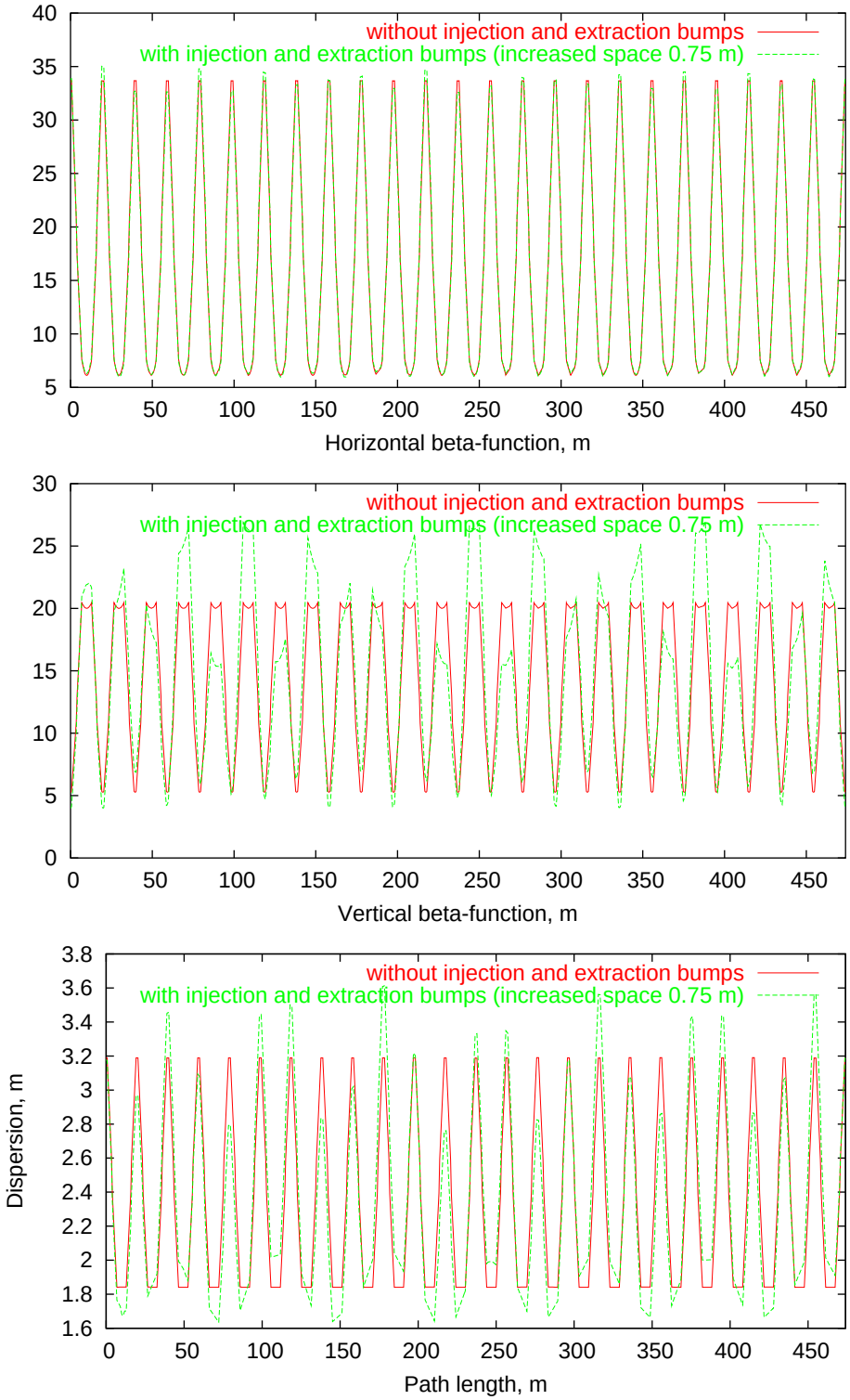

Figure 17: Fermilab Booster horizontal (top), vertical (middle) β functions and horizontal dispersion (bottom) at injection without injection and extraction bumps, and with injection bump and with DogLeg bump at Long03 and Long13 with space between magnets increased by 0.75 m.

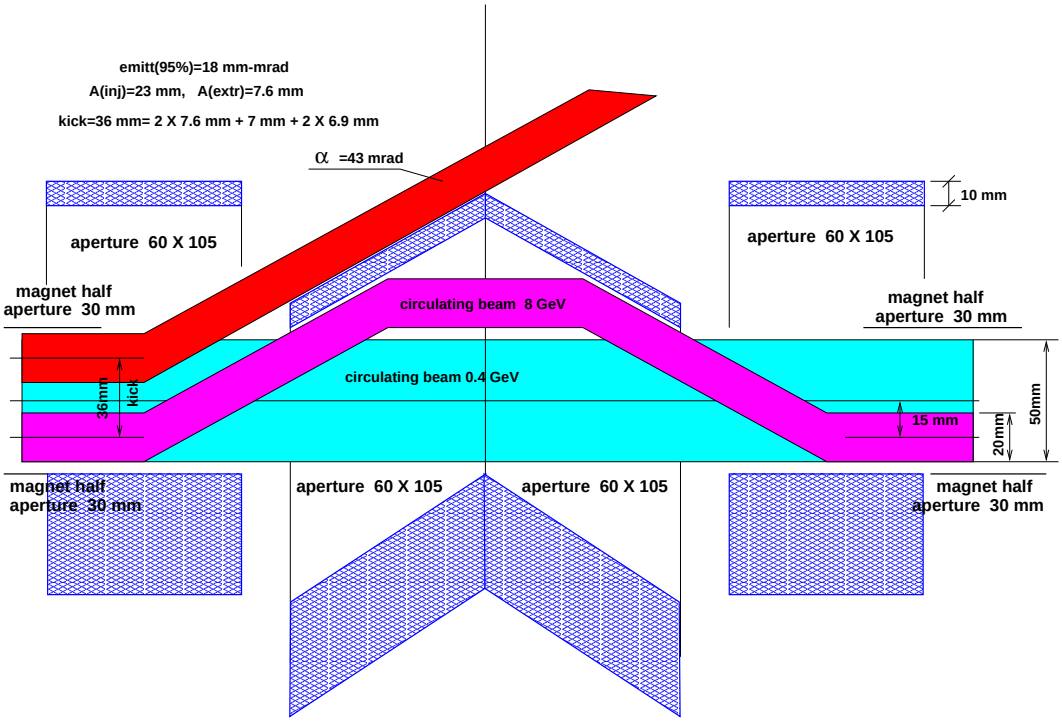

Figure 18: New extraction bump at Long-03 and Long-13 straight sections. The septa is outside of the main magnet aperture.

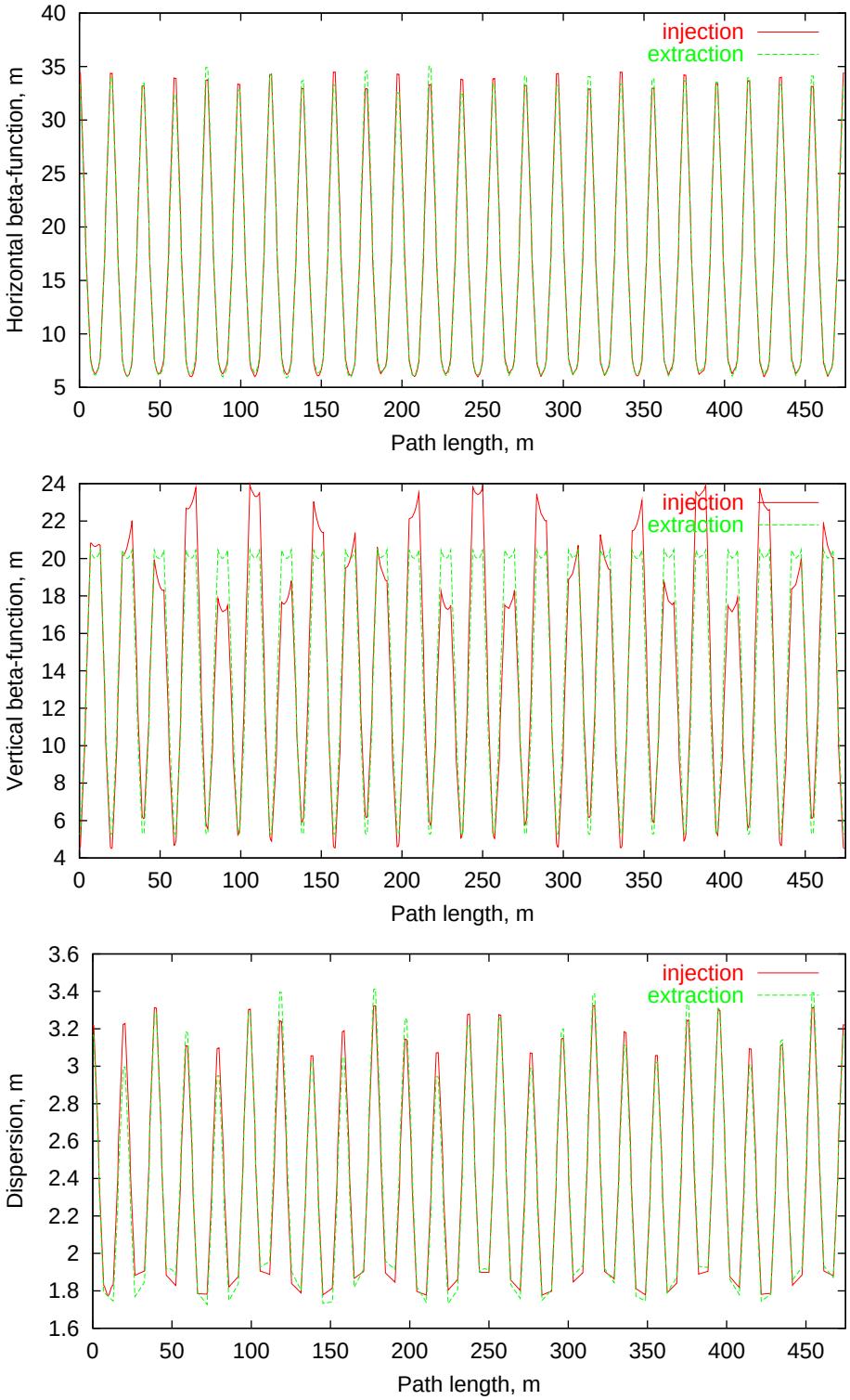

Figure 19: Fermilab Booster horizontal (top), vertical (middle) β functions and horizontal dispersion (bottom) at injection and extraction for "version 7d" - with new injection scheme and with a new extraction bump at Long03 used only at the top energy.

3 Chromaticity modeling

The present setting of the chromaticity during the cycle is somewhat confusing. For instance, the horizontal chromaticity is positive below transition, which could cause the head-tail instability that has not been seen. It is decided to try other chromaticity ramp curves by compiling a spreadsheet relating the sextupole setting with the machine chromaticity. There are four major contributors to the chromaticity: lattice (main quads), dogleg (edge focusing), sextupole of the main magnets and chromaticity correction sextupole.

$$\xi = \xi_{lattice} + \xi_{dogleg} + \xi_{main\ magn.sext.} + \xi_{chrom.\ corr.sext.} \tag{7}$$

The direct contribution form the dogleg is small. However, it has big impact on the chromaticity, because it changes the local beta and dispersion functions at the chromaticity sextupoles. One unknown parameter in this equation is the sextupole component of the main magnets, which comes not only from the body but also from the ends. In order to get a reliable value of this parameter, a "blind check" method was applied. Two teams, one working on the chromaticity and another on the field, carried out the measurements independently without communication between them. The results were then put on the table for a comparison. The agreement is very good, as listed in Table 2. It is seen that the ends compensate the body sextupole of the F magnet almost perfectly, but nearly doubles that of the D magnet.

Magnet type	Body only	Body + Ends field meas.	Body + Ends chrom meas.
F	0.026	0.0045	-0.003
D	-0.021	-0.0413	-0.0454

Table 2: Sextupole component of the main magnets.

4 Acknoledgement

This study is a collaboration involving physicists and engineers from the Beam Physics Department, Proton Source Department, Operation Department, Technical Division and Computer Division. The authors would like to express their thanks to the following people for their help and stimulation discussions: J. Amundson, J. DiMarco, M. Foley, D. Harding, J. MacLachlan, E. Malamud, E. McCrory, E. Prebys, P. Schlabach, P. Spentzouris, M. Syphers, L. Teng, R. Tomlin, D. Wolff and X. Yang.

References

[1] http://www-bd.fnal.gov/pdriver/booster/

[2] W. Chou, A. Drozhdin, P. Lucas, F. Ostigay, FNAL, Batavia, IL 60510, USA, "Fermilab Booster Modeling and Space Charge Study", FERMILAB-Conf-03-08?, Presented to PAC2003.